ELSEVIER

Earth and Planetary Science Letters 176 (2000) 147–156

EPSL

www.elsevier.com/locate/epsl

Long-term cosmogenic ^{3}He production rates (152 ka–1.35 Ma) from ^{40}Ar/^{39}Ar dated basalt flows at 29°N latitude

Tibor J. Dunai *, Jan R. Wijbrans

Isotopengeologie, Faculteit der Aardwetenschappen, Vrije Universiteit, De Boelelaan 1085, 1081 HV Amsterdam, The Netherlands

Received 3 June 1999; received in revised form 1 December 1999; accepted 1 December 1999

Abstract

A set of time integrated cosmogenic ^{3}He production rates in olivines for the last 1.35 Ma are presented. We investigated three basaltic lava flow tops from Lanzarote, Canary Islands, Spain. The ^{40}Ar/^{39}Ar ages determined for those basalt flows by incremental laser heating of leached groundmass samples are 152 ± 26 ka, 281 ± 19 ka and 1.35 ± 0.01 Ma (± 2σ). Three or four different olivine phenocryst samples have been analyzed from each flow for their cosmogenic ^{3}He abundances. The resulting ^{3}He production rates in olivine at sea level at 29° latitude are 82 ± 14 and 82 ± 8 atoms g^{-1} a^{-1}, as obtained from the 152 ka and 281 ka old flows, respectively. Considering effects of erosion on the 1.35 Ma old flow we find that the production rate of 82 ± 8 atoms g^{-1} a^{-1} is consistent with the cosmogenic ^{3}He production during the last 1.35 Ma. There appears to be a 14% discrepancy between previously published production rates derived at higher latitudes and altitudes if the scaling factors of Lal are used to compare results. This discrepancy is greatly reduced, however, if the revised scaling factors of Dunai (this issue) are applied. Using the new scaling factors we derive a production rate for cosmogenic ^{3}He in olivine at sea level and high latitudes (> 60°) of 118 ± 11 atoms g^{-1} a^{-1} (± 2σ). The correspondingly revised value of Cerling and Craig, and Ackert et al.) is 123 ± 6 atoms g^{-1} a^{-1} (± 2σ). The mean value of these two calibrations is 121 ± 6 atoms g^{-1} a^{-1} (± 2σ). We suggest that the production rate of 121 ± 6 atoms g^{-1} a^{-1} at sea level and high latitudes may be applied to the complete time range where paleomagnetic data indicate that there was no long-term averaged intensity variation in the Earth's magnetic field, i.e. over the last 10 Ma.

Keywords: cosmogenic elements; helium; production; rates; magnetic field; exposure age

1. Introduction

The reliability of application of in-situ produced cosmogenic nuclides to dating of exposed surfaces critically depends on the accurate knowledge of production rates [6–8]. However, the production rates vary spatially, and through time. The spatial dependence is the combined effect of atmospheric depth, through absorption of primary and secondary cosmic rays (e.g. [9]), and the influence of the geomagnetic field which deflects the charged primary cosmic rays as a function of its horizontal field strength and inclination

* Corresponding author. Tel.: +31-20-4447398; Fax: +31-20-6462457; E-mail: dunt@geo.vu.nl

0012-821X/00/$ – see front matter
PII: S0012-821X(99)00308-8

[10,11]. The temporal variation is mostly an expression of the secular variation of the geomagnetic field (e.g. [12]). Changes in the intensity of the Earth's magnetic field have been significant throughout the past 800 ka [13]. The last 15 ka, especially the last 10 ka, were characterized by 25–30% higher average virtual axial dipole moments (VADM) [5,13] as compared to the long-term average VADM (>100 ka) [13]. So far most calibrations of in-situ cosmogenic nuclide production rates are from surfaces younger than 18 ka (e.g. [8,14–16] and refs. in [1]). Thus using these production rates for dating of old surfaces the ages may have a substantial bias and hence considerable uncertainties.

We determined the cosmogenic ^{3}He concentration in olivines from three exposed lava flow tops on Lanzarote, Canary Islands, Spain. The same flows were also dated with the ^{40}Ar/^{39}Ar-incremental heating method. The resulting production rates for ^{3}He in olivine cover the time range 150–280 ka and based on our experimental data it is shown they can be extended to ages >1.35 Ma.

2. Analytical methods

Incremental heating ^{40}Ar/^{39}Ar age determinations were performed on leached basaltic groundmass samples using an argon laser probe combined with a MAP 215-50 mass spectrometer [17]. Sample preparation, acid leaching and mass spectrometry are described in [18]. Plateau ages were calculated as weighted means using $1/\sigma^2$ as weighting factor [19] and argon isotope isochron ages as YORK2 least-square fits with correlated errors [20] on the basis of Taylor Creek Rhyolite (TCR) sanidine as flux monitor (28.34 Ma) [21].

Helium isotope determinations were performed on high-purity olivine phenocryst separates ($>98\%$), both utilizing a double vacuum furnace with Mo-crucible and -liner (extraction temperature 1850°C) and a crushing device interfaced to a purification line and a VG-5400 noble gas mass spectrometer. The purification steps and analysis of noble gases are described in [22].

The major element compositions of the olivine phenocrysts were determined by multiple spot analysis using a JEOL® JSM-6400 microprobe. U and Th concentrations of the basalts were determined by INAA (Activation Laboratories Ltd., Ancaster, Ont., Canada).

3. Sample description

Lanzarote chosen as Quaternary volcanism on this island provides a wealth of suitable surfaces, which are mostly well preserved in the prevailing arid climate. The presence of olivine in all our samples indicates that rates of chemical weathering were low throughout the entire exposure history ([23] and refs. therein). Furthermore the climatic conditions eliminate the need to consider effects of snow cover that might be a problem for sites at higher latitude [8]. Preserved marine shorelines [24] indicate that vertical neo-tectonic movements were small during the Quaternary. The low latitude of Lanzarote (29°S) provides a high sensitivity to temporal changes of the geomagnetic field, which is ideal for the purpose of our study.

3.1. Tahiche

The east slope of Tahiche volcano, located about 5 km north of Arrecife (Sheet Arrecife 48-36, UTM grid coordinates: 28RTF432099), was sampled. The sampling sites are at 195–200 m altitude. The lava flow tops at this location are mostly well preserved. Care has been taken to stay away from human structures (dry stone walls) and depressions that accumulated soil. Sampled sites are local highs. From the preservation of small scale flow top features we estimate the overall erosion of the sampling sites as less than 2–4 mm. Thickness of samples was ~ 5 cm. Vesicularity of the samples is 15–20%. As the neutron flux in the uppermost 10 g/cm^2 of the solid Earth is virtually constant [25], the production of cosmogenic nuclides in the uppermost ~ 5 cm of the sampled flow is likewise constant. Therefore no depth correction is necessary. Samples TA1–3 were taken about 10 m from each other. Topographic shielding at all three sites is less than 1% and is corrected for. The olivine

Table 1
$^{40}Ar/^{39}Ar$-incremental heating results of leached groundmass samples

Sample	Weight (mg)	Incremental heating (plateau ages)				Inverse isochron[a]		
		n	MSWD	^{39}Ar %	Age (ka) $\pm 2\sigma$	MSWD	$^{40}Ar/^{36}Ar_{int}$ $\pm 2\sigma$	Age (ka) $\pm 2\sigma$
TA1	127	3	0.96	65.1	175 ± 11	0.46	330 ± 60	130 ± 70
TA2	130	3	1.1	60.1	260 ± 16	2.35	300 ± 150	240 ± 330
TA3	119	4	1.54	83.6	152 ± 26	1.82	292 ± 11	180 ± 110
best TA		(TA3)			152 ± 26 ($\pm 2\sigma$)			
AFB1	113	3	1.33	67.0	272 ± 24	2.74	290 ± 80	320 ± 510
AFB2	116	no plateau obtained				–	–	–
AFB3	105	3	2.24	68.9	289 ± 29	4.49	290 ± 120	290 ± 330
mean age AFB		(AFB1 and 3)			281 ± 19 ($\pm 2s_e$)			
MRB1	118	no plateau obtained				–	–	–
MRB2	125	5	0.63	88.4	1336 ± 15	0.80	299 ± 22	1332 ± 35
MRB3a	137	3	1.96	67.2	1336 ± 19	0.15	306 ± 11	1314 ± 27
MRB3b	120	5	1.43	77.2	1365 ± 17	0.74	293 ± 2	1373 ± 17
mean age MRB		(MRB2, 3a and 3b)			1346 ± 10 ($\pm 2s_e$)			

n denotes number of steps included in calculation of plateau ages. ^{39}Ar% gives the % of ^{39}Ar released in the steps included in the calculation. $^{40}Ar/^{36}Ar_{int}$ is the $^{40}Ar/^{36}Ar$ ratio of the intercept. The best representation of the age of the TA flow is the age obtained from sample TA3. Mean ages for the AFB and MRB flows are calculated from plateau ages that agree within 2σ. The error quoted for those flows is the mean error (s_e) of the mean age at the 95% confidence level. The full data sets are given as an **EPSL Online Background Dataset**[1].

[a]Inverse isochrons are calculated over the steps that are part of the plateaus.

phenocrysts from the Tahiche flow are $Fo_{82\pm4}$. The whole rock has U and Th concentrations of 0.9 ± 0.1 ppm and 3.1 ± 0.2 ppm, respectively.

3.2. Atalaya de Femes

A lava flow covering a very shallow dipping flat plain ($\sim 0.5°$) about 4 km west of the peak of Atalaya de Femes volcano was sampled (sheet Femes 47-37, 28RFS146992). The sampling site is at 35 m altitude. The lava flow tops are well preserved as thin blocks. However, the individual flow top blocks are part of a desert pavement. All blocks are in original orientation. Estimated overall erosion of flow top features at the sampling sites is less than 2–4 mm. Sampled blocks were ~ 5 cm thick. Vesicularity of the samples is 10–25%. Similar to the samples from the Tahiche flow no depth correction is necessary. For the interpretation of the plain the genetic model for desert pavement evolution tested by Wells and coworkers [26] is applied. According to this model the pavement clasts are vertically uplifted by windblown dust. The model predicts that the pavement clasts are continuously exposed since the formation of the underlying lava flow. To test the validity of this model for the sampling site four samples, AFB1–4, were taken about 5 m apart from each other. Topographic shielding is less than 0.5%. The olivine phenocrysts from the Atalaya de Femes flow are $Fo_{83\pm2}$. The whole rock has U and Th concentrations of 0.5 ± 0.1 ppm and 1.7 ± 0.1 ppm, respectively.

3.3. Montanarroja

Remnants of a lava flow on the plain about 2 km NW of the peak of Montanarroja volcano were sampled (sheet Femes 47-37, 28RFS103948). The sampling site is at 30 m altitude. Samples were taken from the uppermost 5 cm of highly vesicular, edge-rounded boulders. The boulders in the sampled area were all in original position, i.e. vesicularity increased markedly towards the top of the boulders. By comparison with vesicular sequences in older lava flows exposed along the nearby coast (~ 1 km) it is estimated that the

[1] http://www.elsevier.nl/locate/epsl;
mirror site: http://www.elsevier.com/locate/epsl

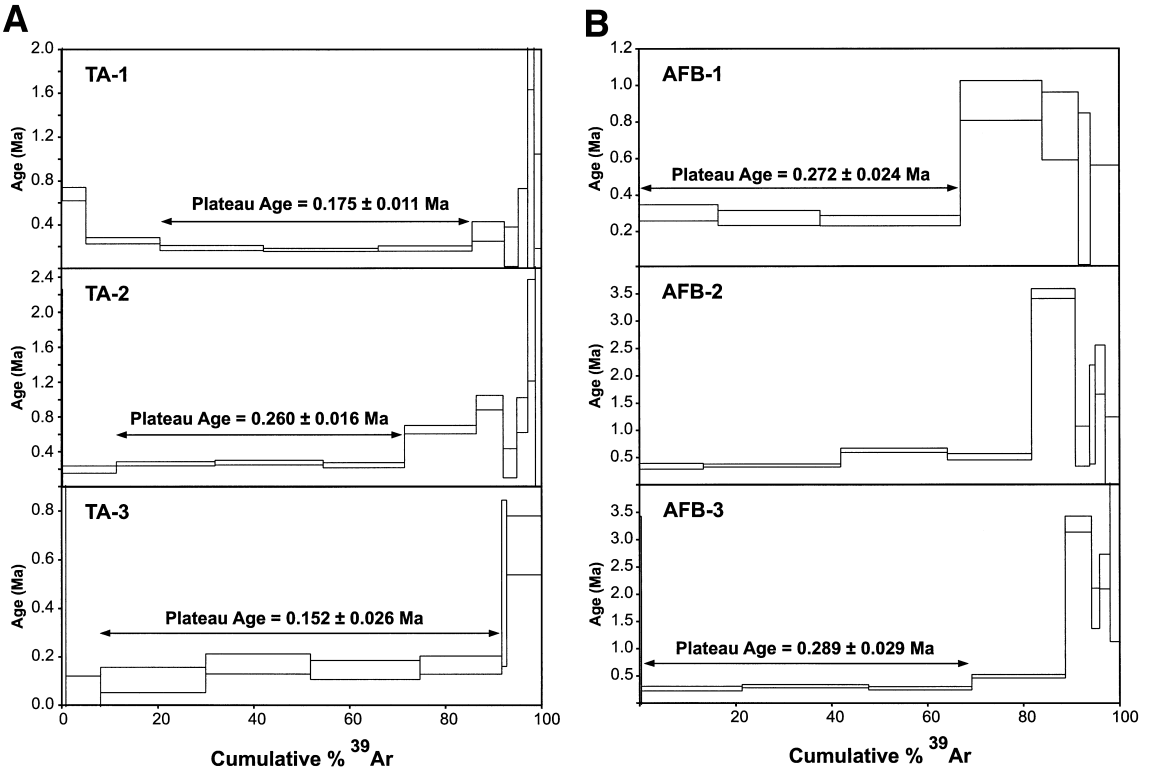

Fig. 1. $^{40}Ar/^{39}Ar$ ages plotted vs. the amount of ^{39}Ar, with calculated plateau ages. A: Tahiche flow samples. B: Atalaya de Femes flow samples. C: Montanarroja flow samples. Discussion is given in the text. Errors throughout the figures are 2σ.

total vertical erosion of the boulders sampled can be on the order of 20 cm. Vesicularity of the samples is 15–20%. Assuming that the flow eroded by more than 5 cm the samples were corrected for the decrease of cosmogenic production with depth. The presence of ephemeral stream beds in the vicinity (100 m) indicate the possibility of run off erosion of the lava flow top in the past. Samples from three boulders were taken (MRB1–3), about 5 m apart from each other. Topographic shielding is less than 0.5%. The olivine phenocrysts from the Montanarroja flow are $Fo_{84\pm1}$. The whole rock has U and Th concentrations of 0.7 ± 0.1 ppm and 2.8 ± 0.2 ppm, respectively.

4. Results

The $^{40}Ar/^{39}Ar$ age results are summarized in Table 1 and Fig. 1. The calculation of plateau ages required data from at least three consecutive temperature steps, which together comprise more than 60% of the total ^{39}Ar release, with each contributing step yielding an age within two standard deviations of the mean age [27]. All plateau ages obtained are identical at the 95% confidence level to the inverse isochron ages calculated from the same steps. Intercepts of the inverse isochrons are atmospheric at the 95% confidence level. A plateau is considered acceptable when the MSWD calculated for the plateau is close to 1.0 and < 2.5 [28]. When analyses of multiple samples from a single flow yielded a significant range in ages, the lowest acceptable plateau age was chosen because most processes causing scatter in the age of such young rocks will tend to increase the apparent age [29]. Hence we argue that the youngest plateau age is the best representation of the age of extrusion of the lava flow. In case we would miss to spot a trapped component, the calculated ages would be biased towards higher

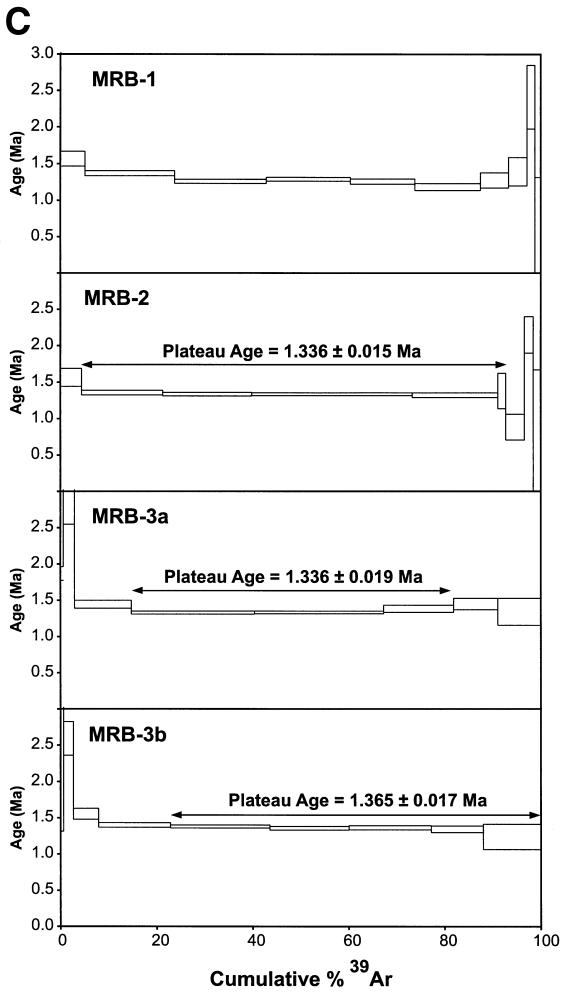

Fig. 1 (*continued*).

values and calculated production rates could be slightly underestimated.

The plateau ages of the three samples from the Tahiche flow give an age range between 152 and 260 ka. The high age of sample TA2 is due to an unresolved contribution of trapped magmatic argon which is probably hosted in small olivines in the groundmass that evaded handpicking. Also for sample TA1 a trapped magmatic component may not be excluded ($^{40}Ar/^{36}Ar_{int} = 330 \pm 60$, $\pm 2\sigma$). It also shows a disturbed plateau with evidence for trapped argon in both the low *and* high temperature steps. Thus the age obtained from the three intermediate steps may be too high. The steps from which the plateau age of sample TA3 was calculated yield, however, a well defined atmospheric intercept for the inverse isochron ($^{40}Ar/^{36}Ar_{int} = 292 \pm 11$, $\pm 2\sigma$, Table 1). Thus for this sample a trapped magmatic component can be excluded for the four consecutive steps used for the plateau age. The value of 152 ± 26 ka is therefore chosen as preferred age for the Tahiche flow and is later used for calibration of production rates.

For two of three analyzed samples of the Atalaya de Femes flow, plateau ages could be obtained that are indistinguishable. The MSWD values of both plateau ages are acceptable (i.e. < 2.5 [28]). Regression of the plateau steps does not indicate a trapped Ar component different from

Table 2
Helium heating results

Sample	Weight (mg)	$^3He/^4He$ crush ($\times 10^{-6}$) $\pm 2\sigma$	$^3He/^4He$ melting ($\times 10^{-5}$) $\pm 2\sigma$	^4He atoms/g ($\times 10^{12}$) $\pm 2\sigma$	$^3He^a_{cos}$ atoms/g ($\times 10^6$) $\pm 2\sigma$	Prod. rate[b] at sea level 29° lat. (atoms g^{-1} a^{-1}) $\pm 2\sigma$
TA1	317	–	1.41 ± 0.07	2.54 ± 0.04	13.7 ± 2.6	78 ± 20
TA2	284	8.97 ± 0.55	1.66 ± 0.05	1.87 ± 0.03	14.7 ± 1.9	85 ± 17
TA3	301	–	3.07 ± 0.11	0.634 ± 0.009	14.3 ± 1.0	82 ± 14
			mean ($\pm 2s_e$)		14.2 ± 1.0	82 ± 14
AFB1	296	–	2.00 ± 0.03	2.13 ± 0.03	24.1 ± 1.5	85 ± 12
AFB2	325	–	2.02 ± 0.06	1.99 ± 0.03	23.2 ± 1.4	82 ± 12
AFB3	288	8.93 ± 0.18	1.43 ± 0.04	4.04 ± 0.06	22.3 ± 2.0	79 ± 15
AFB4	273	–	1.33 ± 0.04	5.30 ± 0.08	23.9 ± 2.5	84 ± 18
			mean ($\pm 2s_e$)		23.4 ± 0.9	82 ± 8
MRB1	212	–	6.14 ± 0.15	1.63 ± 0.02	92.2 ± 4.8	68 ± 7
MRB2	245	–	7.87 ± 0.18	1.11 ± 0.02	84.3 ± 4.3	63 ± 6
MRB3	261	9.40 ± 0.47	7.12 ± 0.16	1.50 ± 0.02	100.5 ± 4.7	73 ± 7
			mean ($\pm 2s_e$)		92.3 ± 2.7	69 ± 4

Errors include the reproducibility of calibrations throughout the period the measurements were performed (abundances ± 1%, ratios ± 2%; $\pm 2\sigma$) and the uncertainty of the amount of calibration gas ($\pm 1\%$, $\pm 2\sigma$), all errors are fully propagated. Mean $^3He_{cos}$ concentrations are given with twice the mean error as uncertainty. The mean production rates are calculated using the best/mean ages in Table 1 and the mean $^3He_{cos}$ concentrations. The error quoted is the mean error (s_e) of the mean production rate at the 95% confidence level. See text for further explanation.

[a]Corrected for magmatic helium and implanted ^4He, the MRB samples are also depth corrected.

[b]To calculate the production rate at sea level at 29° latitude an attenuation mean path length (Λ) of 145 g/cm^2 was used [4].

air. For the calibration of production rates, the mean of the two ages of 281 ± 19 ka is used as the preferred age of the Atalaya de Femes flow.

For three samples and a duplicate (MRB3a+b) of the Montanarroja flow plateau ages could be obtained. The ages range between 1.34 and 1.37 Ma. The preferred age is 1.35 ± 0.01, calculated from the arithmetic mean of three measurements.

The helium results are summarized in Table 2. For each lava flow one olivine sample has been crushed to analyze the magmatic helium component trapped in fluid inclusions. This helium component is characterized by $^3He/^4He$ ratios between 6.42 Ra and 6.76 Ra (where Ra is the atmospheric ratio of $1.39 \cdot 10^{-6}$). The helium released by fusion experiments has in all cases a higher $^3He/^4He$ ratio when compared to that of the corresponding trapped component. Between 30–85% of the ^3He in the samples is cosmogenic ($^3He_{cos}$).

To calculate the contribution of cosmogenic ^3He it is necessary not only to correct for the trapped component, but also consider the effect that implanted ^4He has on the correction. Although the analyzed olivine phenocrysts have low U and Th concentrations of < 0.05 ppm and < 0.15 ppm, respectively (using whole rock concentrations and distribution coefficient < 0.05 [30]), the contribution of radiogenic ^4He implanted as α-particles from the surrounding host rock can be significant. If this implanted ^4He is erroneously attributed to the trapped magmatic component, the magmatic ^3He contribution will be overestimated. Consequently the calculated cosmogenic ^3He concentration will be too low. To estimate the contribution of implanted ^4He we assume a spherical geometry of the olivine phenocrysts and use a slightly modified equation from [31]:

$$F_{\text{implanted}} = 3S/4R + S^3/16R^3$$

where S is the mean stopping range of α-particles, R the radius of the sphere and $F_{\text{implanted}}$ is the fraction of ^4He implanted into the sphere relative to the ^4He produced in an identical volume of host rock. The equation is valid for $R \gg S$. The mean stopping ranges for α-particles in materials with densities similar to olivine and basalt are 19.7, 22.8 and 22.5 μm, for ^{238}U, ^{235}U and ^{232}Th, respectively [31]. As the radius of the

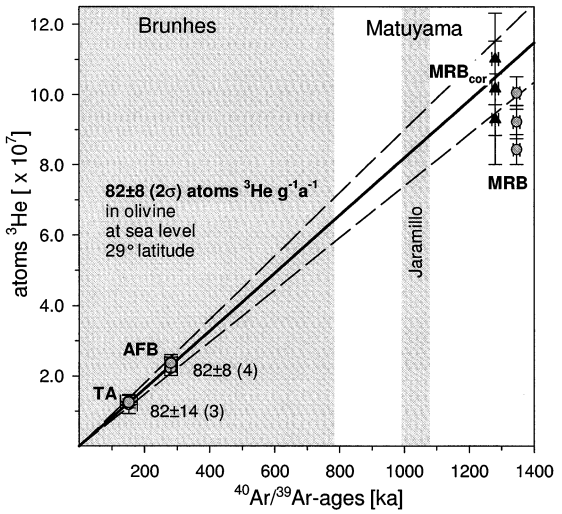

Fig. 2. $^3He_{cos}$ concentration of olivine phenocrysts corrected for altitude plotted vs. the $^{40}Ar/^{39}Ar$ age of the host basalt. Numbers to the left of TA and AFB sample clusters give the mean production rate of $^3He_{cos}$ derived for those clusters. The solid line illustrates the mean production rate of the TA and AFB sample clusters (82 ± 8 atoms g^{-1} a^{-1}), the stippled line marks the 2σ error envelope. MRB_{cor} (▲) denotes MRB samples corrected for effects of erosion (see text), the larger error bars for the corrected samples are the result of the uncertainty on the assumed amount of erosion. Please note that the points of MRB_{cor} are shifted to the left for reasons of clarity only. Their $^{40}Ar/^{39}Ar$ age is of course the same as for uncorrected MRB samples. The shaded areas denote the duration of geomagnetic polarity chrons and subchrons in the calibration time range. Errors throughout the figure are 2σ.

spheres we take 150 ± 50 μm as obtained from thin sections. Using the above equation we calculate for samples TA, AFB and MRB that 5.9×10^{10}, 6.8×10^{10} and 5.0×10^{11} atoms ^{4}He g^{-1} were implanted, respectively. The relative contribution to the overall ^{4}He in the olivines is 2–9% for TA samples, 1–3% for AFB samples and 30–45% for MRB samples. Considering the implanted ^{4}He, the calculated concentrations of $^3He_{cos}$* (Table 2) are 3–5% higher than those obtained when implantation is ignored.

5. Discussion

The $^3He_{cos}$ concentrations in TA and AFB samples cluster tightly around mean values of $14.2 \pm 1.0 \times 10^6$ and $23.4 \pm 0.8 \times 10^6$ atoms/g, respectively (Table 2). Therefore, the assumption of a simple exposure history for TA samples and using the model of [26] for desert pavement evolution for AFB samples (see Section 3) are justified. Consequently the $^3He_{cos}$ concentrations obtained for those samples can be used for production rate calibration. The $^3He_{cos}$ concentrations in the MRB samples, however, scatter significantly. This is the result of variable erosion that affected the MRB samples as was noted from the field evidence. Taking those effects into account, the results of the MRB samples, however, can be used to test whether the calculated production rates of the younger samples are compatible with observed $^3He_{cos}$ concentrations.

Combining the $^{40}Ar/^{39}Ar$ ages with the $^3He_{cos}$ concentrations we calculate production rates of $^3He_{cos}$ in olivine. To obtain production rates at sea level an attenuation mean path length Λ of 145 g/cm^2 is used [4]. The resulting mean production rates are 82 ± 14 and 82 ± 8 atoms ^{3}He g^{-1} a^{-1} for sample clusters TA and AFB, respectively (Table 2 and Fig. 2). Thus the production rates are indistinguishable which supports the reliability of the calibration. The mean virtual axial dipole moments (VADM) over the last 158 ka and 276 ka differ by less than 1% [13]. Thus the production rates must be indistinguishable. Therefore we treat means of sample clusters TA and AFB as samples from the same population and derive a *mean production rate for the last* 276 ka *of* 82 ± 8 *atoms* ^{3}He g^{-1} a^{-1} *in olivine at sea level and* 29° *latitude*.

The production rates calculated for samples MRB1–3 are mostly lower than the mean value of 82 ± 8 atoms g^{-1} a^{-1}, only sample MRB3 (73 ± 7 atoms g^{-1} a^{-1}) overlaps with the production rate obtained from the two younger flows TA and AFB. When considering the erosion deduced for the sampled surfaces ($\sim 20 \pm 5$ cm; assuming linear erosion over 1.35 Ma), however, the picture changes and all three samples overlap with the mean production rate calculated from the TA and AFB flows (Fig. 2). *The correction for erosion is inevitably paired with an increased uncertainty. Although, even if the estimates of erosion would vary by a factor of two the overlap still persists.*

Therefore, we conclude that the production rates calculated for the last 281 ka may be extended to 1.35 Ma. The apparent constancy of time averaged cosmogenic production rates over the last 1.35 Ma years implies that the average intensity of the geomagnetic field has been relatively constant, despite of the combined effects of three major reversals that occurred during the time span of the current calibration (Fig. 1). This finding is in perfect agreement with paleointensity data of the geomagnetic field over the last 10 Ma indicating that intensities of normal and reverse polarities are indistinguishable and long-term mean values are similar ([5] and refs. therein). *Therefore we suggest that further extension of the calibration range beyond* 1.35 Ma *is justified up to at least* 10 Ma.

We now compare our long-term production rate of 82 ± 8 atoms ^{3}He g^{-1} a^{-1} obtained at 29° latitude with the only other long-term calibration available to date [2]. In the study of [2] clinopyroxene phenocrysts from 47°S latitude from a 128 ka old basalt flow were analyzed. The authors suggest that the production rate of [1] of 115 ± 6 ($\pm 2\sigma$) atoms ^{3}He g^{-1} a^{-1} for olivines at sea level high latitudes ($> 60°$), derived from ~ 18 ka surfaces, is consistent with their results. We take the view, however, that the agreement is fortuitous as the mean virtual axial dipole moment (VADM) of the Earth's magnetic field was 1.3 times stronger over the last 18 ka as compared to the last 128 ka [13]. Thus the average production rates at the site of calibration of [1] were 9% lower, assuming the axial dipole assumption is true (using the cut off energy cosmic ray flux relation in [4]). However, also the axial dipole assumption for young samples < 20 ka is problematic [5,8] and deviations from that assumption have a strong effect as to the high sensitivity of cosmic ray flux to the inclination of the geomagnetic field [10,32]. Resolving this problem for the young calibration sites used by [1] is beyond the scope of this paper and we will limit the comparison to the results of [2] which are unproblematic with respect to the axial dipole assumption. The mean VADM over the last 128 ka was only 1.5% lower than average over the 152 ka or 281 ka [13], the time ranges relevant for the current calibration. Thus the production rates at 47°S, the latitude of the calibration site of [2] were virtually the same over the last 128 ka as over the 152 ka or 281 ka.

Using the scaling factors of [3] and production rate of 115 ± 8 ($\pm 2\sigma$) atoms ^{3}He g^{-1} a^{-1} [2] we calculate that at sea level and 29° latitude the production rate for ^{3}He in olivine should be 94 ± 5 ($\pm 2\sigma$) atoms g^{-1} a^{-1}. However, the value obtained by us is 14% lower. Thus, assuming that our data set is valid, either the production rate of 115 ± 6 atoms g^{-1} a^{-1} ($\pm 2\sigma$) or the scaling factors of [3] do not well describe the cosmogenic production at the sampling sites at 29° and 46°.

A recent reevaluation of scaling factors [4] showed that, when using the scaling factors of Lal [3] at sea level and low latitudes (20–40°), the corresponding production rates will be up to 18% too high. At sea level and 29° latitude (sites of the present study) the difference is 17%. Likewise at the location of the calibration site of [2], the production rates will be ~ 7% too high. Thus the apparent discrepancy of 14% between production rates is greatly reduced, ~ 10% difference can be explained by the use of scaling factors of [3] by [2] alone. The remaining difference of 4% is not significant. Both the analytical uncertainty and the uncertainty of scaling factors (~ 2–3%) [4] can account for the difference. We take the good agreement between calibration sites at 47° and 29° latitude as indication that the revised scaling factors of [4] provide a good description of the latitude dependence of cosmogenic nuclide production. For a detailed discussion of the qualitative and quantitative differences between the new scaling factors and those of [3] we refer to [4].

Based on the revised scaling factors of [4] we obtain an integrated production rate of cosmogenic ^{3}He in olivine at sea level and high latitudes of 118 ± 11 atoms ^{3}He g^{-1} a^{-1} ($\pm 2\sigma$). The correspondingly revised value of [2] is 123 ± 6 atoms g^{-1} a^{-1}, $\pm 2\sigma$. We suggest that the mean of these values, 121 ± 6 ($\pm 2\sigma$) atoms g^{-1} a^{-1} at sea level and high latitudes, may be applied to the complete time range where paleomagnetic data indicate that there was no long-term averaged intensity variation in the Earth's magnetic field, i.e. over the last 10 Ma ([5] and refs. therein).

Acknowledgements

This paper benefitted from the constructive reviews of Jozef Mazarik, Brad Singer and Rainer Wieler, which is gratefully acknowledged. We would like to thank of Roel Van Elsas, Lodewijk IJlst and John König for the laborious mineral separation, Volker Wiederhold and Bouk Laçet for preparing the thin sections, Bert Voorhorst for running part of the argon analysis and Wim Lustenhouwer for the microprobe analysis. This is NSG publication number 991104.*[RV]*

References

[1] T.E. Cerling, H. Craig, Cosmogenic ^{3}He production rates from 39°N to 46°N lattitude, western USA and France, Geochim. Cosmochim. Acta 58 (1994) 249–255.

[2] R.P. Ackert, B.S. Singer, H. Guillou, M.D. Kurz, Cosmogenic ^{3}He production rates over the last 125000 years: Calibration against ^{40}Ar/^{39}Ar and unspiked K-Ar ages of lava flows, in: Annual Meeting of the Geological Society of America, GSA, Toronto, 1998, 299 pp.

[3] D. Lal, Cosmic ray labeling of erosion surfaces: in situ nuclide production rates and erosion models, Earth Planet. Sci. Lett. 104 (1991) 424–439.

[4] T.J. Dunai, Scaling factors for production rates of in-situ produced cosmogenic nuclides: a critical reevaluation, Earth Planet. Sci. Lett., 176 (2000).

[5] R.T. Merrill, M.W. McElhinny, P.L. McFadden, The Magnetic Field of the Earth, Academic Press, San Diego, 1998, 531 pp.

[6] T.E. Cerling, H. Craig, Geomorphology and in-situ cosmogenic isotopes, Annu. Rev. Earth Planet. Sci. 22 (1994) 273–317.

[7] M.D. Kurz, D. Colodner, T.W. Trull, R.B. Moore, K. O'Brien, Cosmic ray exposure dating with in situ produced cosmogenic ^{3}He: results from young Hawaiian lava flows, Earth Planet. Sci. Lett. 97 (1990) 177–189.

[8] J.M. Licciardi, M.D. Kurz, P.U. Clark, E.J. Brook, Calibration of cosmogenic ^{3}He production rates from Holocene lava flows in Oregon, USA, and effects of the Earth's magnetic field, Earth Planet. Sci. Lett. 172 (1999) 261–271.

[9] D. Lal, B. Peters, Cosmic ray produced radioactivity on earth, in: S. Flugg (Ed.), Handbook of Physics vol. 46/2, Springer, Berlin, 1967, pp. 551–612.

[10] P. Rothwell, Cosmic rays in the Earth's magnetic field, Phil. Mag. 3 (1958) 961–970.

[11] W.R. Webber, Time variations of low-rigidity cosmic rays during the recent sunspot cycle, in: J.G. Wilson, S.A. Wouthuysen (Eds.), Progress in Elementary Particle and Cosmic Ray Physics vol. 6, pp. 77–243, North Holland Publishing Company, Amsterdam, 1962.

[12] M. Frank, B. Schwarz, S. Baumann, P.W. Kubik, M. Suter, A. Mangani, A 200 kyr record of cosmogenic radionuclide production rate and geomagnetic field intensity from 10Be in globally stacked deep-sea sediments, Earth Planet. Sci. Lett. 149 (1997) 121–129.

[13] Y. Guyodo, J.-P. Valet, Global changes in intensity of the Earth's magnetic field during the past 800 kyr, Nature 399 (1999) 249–252.

[14] P.W. Kubik, S. Ivy-Ochs, J. Masarik, M. Frank, C. Schlüchter, ^{10}Be and ^{26}Al production rates deduced from an instantaneous event within the dentro-calibration curve, the landslide of Köfels, Ötz Valley, Austria, Earth Planet. Sci. Lett. 161 (1998) 231–241.

[15] S. Niedermann, T. Graf, J.S. Kim, C.P. Kohl, K. Marti, K. Nishiizumi, Cosmic-ray-produced 21Ne in terrestrial quartz: the neon inventory of Sierra Nevada quartz separates, Earth Planet. Sci. Lett. 125 (1994) 341–355.

[16] T. Swanson, Determination of 36Cl production rates from the deglaciation history of Whidbey and Fidalgo Islands, Washington, Radiocarbon 38 (1996) 172.

[17] J.R. Wijbrans, M.S. Pringle, A.A.P. Koppers, R. Scheveers, Argon geochronology of small samples using the Vulcaan argon laser probe, Proc. K. Ned. Akad. Wet. 98 (1995) 185–218.

[18] A.A.P. Koppers, 40Ar/39Ar-geochronology and isotope geochemistry of the West Pacific Seamount province, PhD, Vrije Universiteit, Amsterdam, 1998.

[19] J.R. Taylor, An Introduction to Error Analysis, University Science Books, Mill Valley, CA, 1982, 270 pp.

[20] D. York, Least squares fitting of straight line with correlated errors, Earth Planet. Sci. Lett. 5 (1969) 320–324.

[21] P.R. Renne, C.C. Swisher, A.L. Deino, D. Karner, T.L. Owens, D.J. DePaolo, Intercalibration of standards, absolute ages and uncertainties in ^{40}Ar/^{39}Ar dating, Chem. Geol. 145 (1998) 117–152.

[22] M.C. van Soest, D.R. Hilton, R. Kreulen, Tracing crustal and slab contributions to arc magmatism in the Lesser Antilles island arc using helium and carbon relationships in geothermal fluids, Geochim. Cosmochim. Acta 62 (1998) 3323–3335.

[23] M.A. Summerfield, Global Geomorphology, Longman, Essex, 1991, 537 pp.

[24] P. Rothe, Kanarische Inseln, Gebr. Bornträger, Berlin, 1996, 308 pp.

[25] J. Masarik, R.C. Reedy, Terrestrial cosmogenic-nuclide production systematics calculated from numerical simulations, Earth Planet. Sci. Lett. 136 (1995) 381–395.

[26] S.G. Wells, L.D. McFadden, J. Poths, C.T. Olinger, Cosmogenic ^{3}He surface exposure dating of stone pavements, Geology 23 (1995) 613–616.

[27] C.L. Johnson, J. Wijbrans, C.G. Constable, J. Gee, H. Staudigel, L. Tauxe, V.H. Forjaz, M. Salguerio, ^{40}Ar/^{39}Ar ages and paleomagnetism of São Miguel lavas, Azores, Earth Planet. Sci. Lett. 160 (1998) 637–649.

[28] C. Brooks, S.R. Hart, T. Wendt, Realistic use of two-

error regression treatments as applied to rubidium-strontium data, Rev. Geophys. Space Phys. 10 (1972) 551–577.
[29] B.S. Singer, J.R. Wijbrans, S.T. Nelson, M.S. Pringle, T.C. Feeley, M.A. Duncan, Inherited argon in a Pleistocene andesite lava; $^{40}Ar/^{39}Ar$ incremental-heating and laser fusion analyses of plagioclase, Geology 26 (1998) 427–430.
[30] M. Wilson, Igneous Petrogenesis, Unwin Hyman, London, 1989, 466 pp.
[31] K.A. Farley, R.A. Wolf, L.T. Silver, The effects of long alpha-stopping distances on (U-Th)/He ages, Geochim. Cosmochim. Acta 60 (1996) 4223–4229.
[32] P. Rothwell, J. Quenby, Cosmic rays in the Earth's magnetic field, Nuovo Cimento VIII, Serie X (1958) 249–256.